wjert, 2022, Vol. 8, Issue 10, 121-138. Research Article ISSN 2454-695X

World Journal of Engineering Research and Technology
WJERT
www.wjert.org SJIF Impact Factor: 5.924

EXPERIMENTAL AND COMPUTATIONAL INVESTIGATIONS OF CHEMICALLY AND BIOSYNTHESIZED ZNO NANOPARTICLES USING AQUEOUS EXTRACT OF *AZADIRACHTA INDICA* AND THEIR ANTIBACTERIAL ACTIVITIES

[1]Debasmita Das, [1]Biplab Rajbanshi, [1]Paramita Karmakar, [2]Narendra Nath Ghosh, [3]Vijeta Rai, [1]Kangkon Mallick, [1]Mantu Dey, [1]Ankita Shome, [1]Priyanka Roy, [3]Shilpi Ghosh and [1,4]*Mahendra Nath Roy

[1]Department of Chemistry, University of North Bengal, Darjeeling 734013, India.
[2]Department of Chemistry, University of Gour Banga, Malda 732103, India.
[3]Department of Biotechnology, University of North Bengal, Darjeeling 734013, India.
[4]Department of Chemistry, Alipurduar University, Alipurduar, India.

Article Received on 21/08/2022 Article Revised on 11/09/2022 Article Accepted on 01/10/2022

***Corresponding Author**
Mahendra Nath Roy
Department of Chemistry, University of North Bengal, Darjeeling 734013, India.

ABSTRACT

The goal of this study is to compare the optical, morphological, and antibacterial properties of ZnO nanoparticles (NPs) made using chemical and green methods. Fourier transform infraredspectroscopy (FTIR), dynamic light scattering (DLS), Ultraviolet-visible spectroscopy (UV-Vis), Scanning electron microscope (SEM), and X-ray diffraction (XRD) were used to characterize the nanomaterials. Both gram-positive and negative microorganisms were tested for antibacterial activity. Density functional theory (DFT) calculations clearly indicate that quercetin is mainly responsible for the stabilization and reduction of ZnO NPs. Plant-mediated nanomaterials have been found to be a more promising candidate for use in a variety of medicinal and industrial research sectors than chemically synthesized nanoparticles.

KEYWORDS: ZnO nanoparticles; Antibacterial activity; *Azadirachta indica*; Green synthesis.

1. INTRODUCTION

Nanotechnology is a multidisciplinary science that has resulted in the development of a wide range of smart nanomaterials.[1] Plant-based nanomaterials are causing a revolution in modern science, with several applications in the fields of health, cosmetics, electronics, and agriculture.[2] Their nanoscale size (1-100 nm), in particular, improves antibacterial capabilities by absorbing bacterial surfaces.[3] This nanoscale category contains ZnO NPs, which have a wide range of uses in cosmetics, chemical sensors, optoelectronics, single-electron transistors, drug-delivery tissue engineering, antibacterial agents, photocatalysts, and bio-sensing materials. It's a common ingredient in broad-spectrum sunscreen.[4] Furthermore, ZnO NPs have been investigated for their ability to extract Thorium (IV) from aqueous solutions.

Different fabrication approaches are becoming more popular for processing ZnO NPs.[5] Chemical methods have a number of drawbacks, including experimental setup, the employment of additional stabilizing and reducing agents, and poor production of the desired product. The biosynthesis scheme, according to the literature, is a novel alternative to physical and chemical approaches for NPs synthesis. Various nanostructures, such as nanorods, nanotubes, and nanowires are now being prepared from biological sources for various applications.[6,7] In this domain, researchers offered several green sources like fungal biomass, plant extracts, bacteria, algae, and so on for the synthesis of NPs. Multiple phytochemicals and enzymes are found in plant extracts to transform bulk ZnO to nanoscale ZnO. According to the literature, numerous plant extracts were used in the green production of ZnO NPs, including *Trifolium pretense*, *Ocimum basilicum*, *Cassia fistula*, *Aristolochiaindica*, *Limonia acidissima*, *Tabernaemontana divaricate*, *Cochlospermum religiosum*, *Conyza Canadensis*, *Citrusmaxima*, *Boswellia ovalifoliolata*, *Echinacea spp.*, *Salvadora oleoides*, *Sambucus ebulus* and so on.[8-20] *Azadirachta indica* is a highly important medicinal plant that belongs to the Meliaceae family and can be found in India, Pakistan, Nepal, and Bangladesh.[21] The phytochemical screening evaluates the presence of Quercetin, β- sitosterol, polyphenolic flavonoids, saponins, tannins, glycosides, steroids, and alkaloids in neem leaves extract.[22] Neem and its constituents have therapeutic effect and play pivotal role in prevention of various diseases. It is also familiar for anti-inflammatory, anti-tumor, anti-gastric ulcer, anti-pyretic, anti-arthritic, neuroprotective, hypoglycemic properties.[23] When the bio active components of *Azadirachta indica* are trapped with metal NPs these capabilities are enhanced.[1] The inspection of literature revealed the synthesis of silver NPs,

Iron Oxide NPs, Copper NPs, gold NPs, MnO NPs from *Azadirachta indica* extract.[24-28] ZnO NPs, in particular, have sparked a lot of interest. Although prior research had shown that ZnO NPs can be synthesized form neem leaf extract[29-32], the mechanism of interaction was unknown. The interaction of bio components of plant extract with NPs in current communication was disclosed in theoretical investigations, and an eco-friendly approach for the production of ZnO NPs was proposed.

Now a days bacterial diseases has become common threat in tropical regions. Because organic antibacterial agents are extremely sensitive to temperature and pressure during manufacturing, inorganic anti-bacterial agents can be a better alternative to control the microbe. They are generally metallic or metal oxide NPs which are stable at high temperature and pressure.[33] According to literature ZnO NPs inhibit the growth of bacterial pathogens in minimum concentration.[8]

Here, we present a chemical and environmentally acceptable approach for producing ZnO NPs, using zinc nitrate as a precursor, and compare their antibacterial capabilities. This study will improve the biomedical industry's ability to use plant-based NPs.

2. MATERIALS AND METHODS

2.1 Preparation of leaves extract

Fresh and undamaged neem leaves were collected from the premises of University of North Bengal, India. Leaves were cleaned with distill water three times to avoid any contaminations. We then chopped 20g of air dried leaves into smaller pieces and refluxed with 500 ml water for 4 hours. Following that, the resulting solution was filtered by Whatman filter paper No. 1. The yellow colored solution was stored in refrigerator at 4^0C.

2.2 Chemical synthesis of ZnO NPs

The precipitation process was used to make ZnO NPs.[34] Zinc nitrate (Sigma Aldrich, India) become dissolved in distilled water by swirling continuously and heating. At room temperature, a dropwise addition of NaOH (Sigma Aldrich, India) solution to this solution produced a white suspension. After then, it was left to stand for the night. Finally, the white product was centrifuged at 3000 rpm, rinsed with water and alcohol several times, and dried at 400^0C.

2.3 Biosynthesized ZnO NPs using *Azadirachta indica* leaves extract

Water was poured to a 250ml beaker containing 5g $ZnNO_3.6\ H_2O$ salt.[35] Then 10ml leaf broth was added, and the mixture was heated at 70^0C for 2 hours. The pale white color paste was left to heat up at a temperature of 60 ^{0}C. Finally, for characterization, the product was annealed at 400^0C for 2 hours and stored in an airtight bottle.

2.4 Phytochemical screening of *Azadirachta indica*leaves extract

Phytochemical screening was carried out to figure out the active constituents of aqueous extract of neem leaves responsible for reduction and stabilization of bio-synthesized ZnO NPs by standard method.[36]

2.5 Antibacterial assay of ZnO NPs

The comparative analysis of antibacterial potential of the nanoparticles synthesized through green and chemical methods was determined by using the agar well diffusion method. Four different bacterial species were used for the study which including two gram positive bacteria such as *Staphylococcus aureus*and *Bacillus subtilis* and two gram negative bacteria *Shigella Sp.* and *E. Coli*. Before analysis, all the individual stock bacteria were sub-cultured and incubated at 37°C for 24 hours in a nutrient broth medium. Fresh overnight cultures were inoculated on Mueller Hinton Agar (MHA) plates using sterile swabs and allowed to stand for 10 minutes. On the bacterial lawn of MHA plates, sterile cork borer wells of 6 mm diameter were constructed. Each well was filled with 50 µL of 700 g/mL nanomaterials (PE=biosynthesized nanopartiles and CM=chemically synthesized nanoparticles) dissolved in ethanol, with ampicillin (10 g/L) serving as a positive control or reference standard, and ethanol serving as a negative control. The diameters of the inhibition zones around the wells were measured after additional 24 hours of incubation at 37^0C. The following formula was used to obtain the percentage growth inhibition (Eq. 1)

$$\text{Growth Inhibition (\%)} = (B_1 - B_0)/B_1 \times 100 \qquad (1)$$

Where GI (%) = Percent growth inhibition, B_1= Bacteria colony diameter in treatment, B_0 = Bacteria colony diameter in control.

2.6 Computational Details

Ground state geometry optimization of the major compounds of *Azadirachta indica* plant extract (quercetin, β- sitosterol, gedunin), which may be responsible for stabilization of ZnO NPs, were carried out using the density functional theory. All the DFT calculations were

performed utilizing the Gaussian 16 program. Ground state geometry optimization of the major compounds, ZnO NPs and nanocomposites B3LYP/6-31+G(d)/LanL2DZlevel of theory.[37] We choose 6-31+G (d) basis set for all the non-metal atom while LanL2DZis chosen for Zn metal. For representation of the ZnO NPs we choose $Zn_{12}O_{12}$ non-cluster as previous studies revealed that these nanoclusters are highly stable in nature. Vibration frequency analysis were performed to check whether the energy minimized geometries corresponds to the true ground state geometries at the same level of theory. We found no imaginary frequency which confirmed that the geometries are minima on the potential energy surfaces.[38] Finally, by the utilizing the formula, adsorption energies (ΔE_{ads}) for all the composite systems were analyzed (Eq.2)

$$\Delta E_{ads} = E_{ZnO\text{-}NP\text{-}Major\text{-}Compounds} - E_{ZnO\text{-}NP} - E_{Major\text{-}compounds} \quad (2)$$

Where $E_{ZnO\text{-}NP\text{-}Major\text{-}Compounds}$, $E_{ZnO\text{-}NP}$, $E_{Major\text{-}compounds}$ are the total energy of the geometry optimized nanocomposites, free ZnO NPs and the major molecules, respectively.

3. Statistical analysis of ZnO NPs

Pure phase of ZnO NPs were confirmed by different characterization techniques like Fourier Transformed Infrared spectroscopy, X-ray diffraction, UV-Vis spectroscopy. FTIR analysis of NPs was performed in the range of 400-4000 cm^{-1} by Perkin Elmer Spectrum 2. Phase purity and size was evaluated by X-ray diffractometer (Bruker D8 Advance). UV-Vis spectroscopy was used to identify the characteristic surface plasma resonance (Perkin Elmer Lamba 35). The morphological information was gathered form SEM. DLS (Malvern Zetasizer Nano Z was used to evaluate hydrodynamic size and Zeta potential analysis was done to confirm the stability of synthesized ZnO NPs.

4. RESULT AND DISCUSSION

4.1 Optical properties

The synthesis of ZnO NPs was detected using UV-visible spectroscopy. The first sign of NPs creation was a change in the color of the solution from bright yellow to dark brown. Fig. 1(a), 1(b) shows the UV–visible absorption spectra of produced NPs. The unique peak centered around 378 nm and 370 nm indicated that the particles were in the nanometer range and highly photosensitive in nature. Similar results was found in previous studies.[39] The passage of electrons from the valance band to the conduction band causes this peak.[40] There were no other peaks in the spectrum, showing that the products were solely made up of ZnO NPs.[41,42] Because of the higher agglomeration, the green synthesized product has a lesser absorbance.

Temperature is the most critical element in determining the size of NPs. Previous studies havediscovered that high temperatures result in tiny NPs.[43,44] So, we synthesize NPs at a comparatively high temperature of 70^0C.

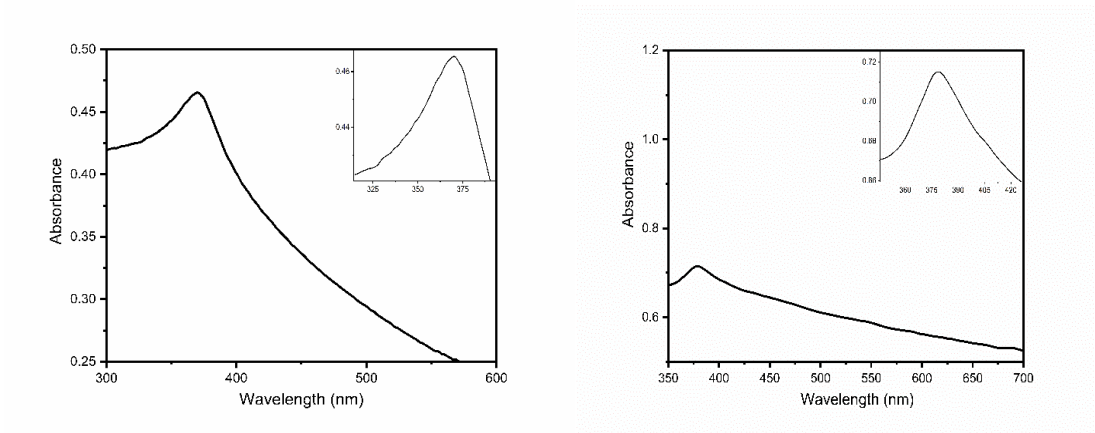

(a) **(b)**

Fig. 1 Absorption spectra of (a) Chemically synthesized (b) Green synthesized ZnO NPs.

4.2 Dynamic light scattering analysis

The particle size distribution was determined using DLS (Fig. 2). A PDI of 0.24 indicates a monodisperse solution. A single prominent peak suggests that the samples are of high quality and homogeneity.[40] Chemically and environmentally produced ZnO NPs had average sizes of 32.67 nm and 24.36 nm, respectively. As a result, bio-mediated NPs have a bigger surface area, and their antibacterial action is higher because they have a greater chance of crossing the bacterial cell membrane and limiting bacterial growth.[45]

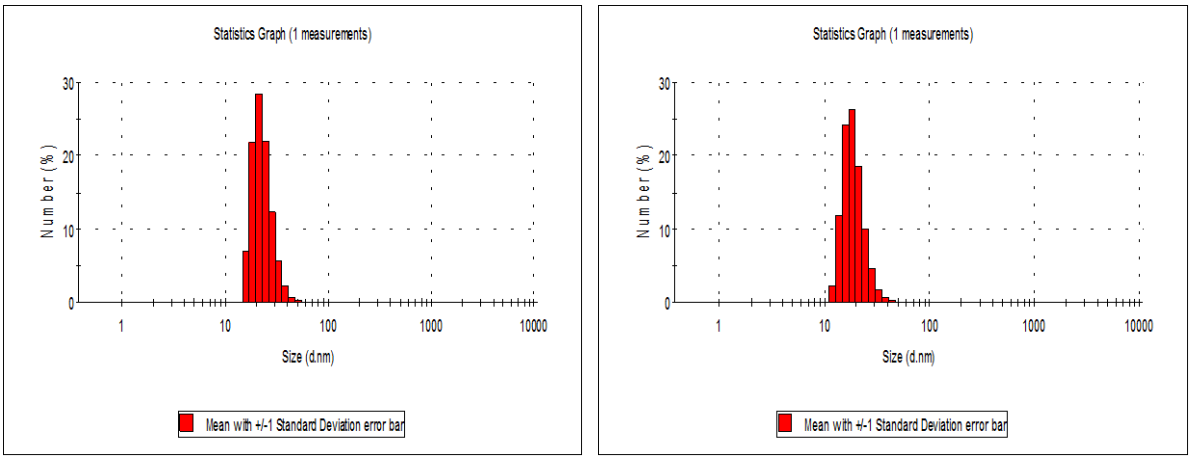

(a) **(b)**

Fig. 2 DLS study of (a) Chemically synthesized (b) Green synthesized ZnO NPs

4.3 FTIR Studies

The purity and characteristics of phytochemical responsible for the synthesis of ZnO NPs were confirmed using infrared analysis (Fig. 3a and 3b). O-H stretching accounts for the broad spectral bands about 3320 cm^{-1}. The absorption band at 2928 cm^{-1} is due to doublet absorption of aromatic aldehyde C-H stretching, which indicates the presence of terpenoid groups in neem leaves extract.[32] The presence of the O-H group, which is derived from the flavonoid group, causes the band at 1492 cm^{-1} to emerge. –C-OC-linkage or –C-O-bands are responsible for the peaks at 1143 cm^{-1}. Alcohol, ketones, aldehyde, carboxylic acid, and flavonoids surround produced NPs, whereas tannin, quercetin, and alkaloids act as capping agents, according to this investigation.=CH2 stretching can be attributed to bands at 898 cm^{-1}[46] and 1634 cm^{-1} stands for C=C bending vibrations. Zn-O stretching vibration is ascribed to the band between 400 and 600 Cm^{-1}.[8] Accordingly, the oxygen or hydroxyl compounds in neem extract give electrons for reducing Zn^{2+} to Zn^{+1} and then to Zinc NPs, while the negative chemical moieties act as stabilisers. As a result, these phytochemicals tend to coat metal oxide layers, which bind with bacterial membrane receivers, boosting anti-bacterial capabilities.[47]

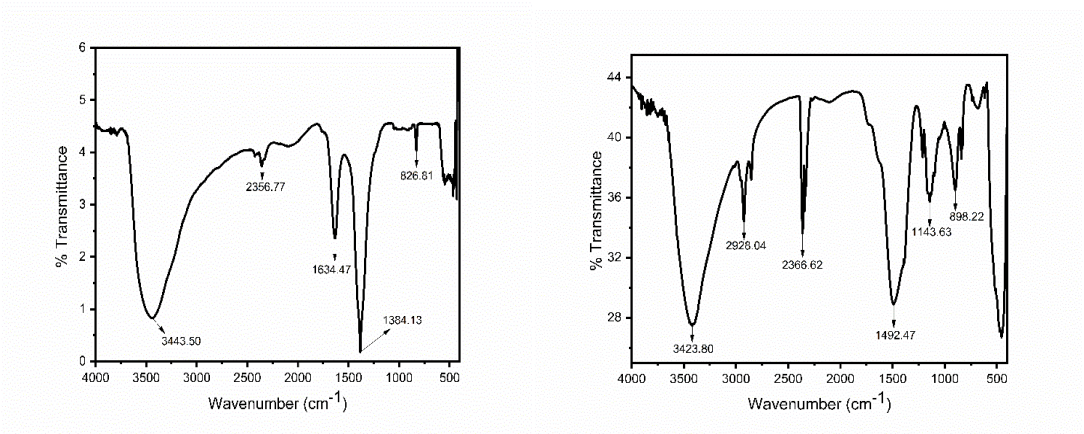

(a) **(b)**

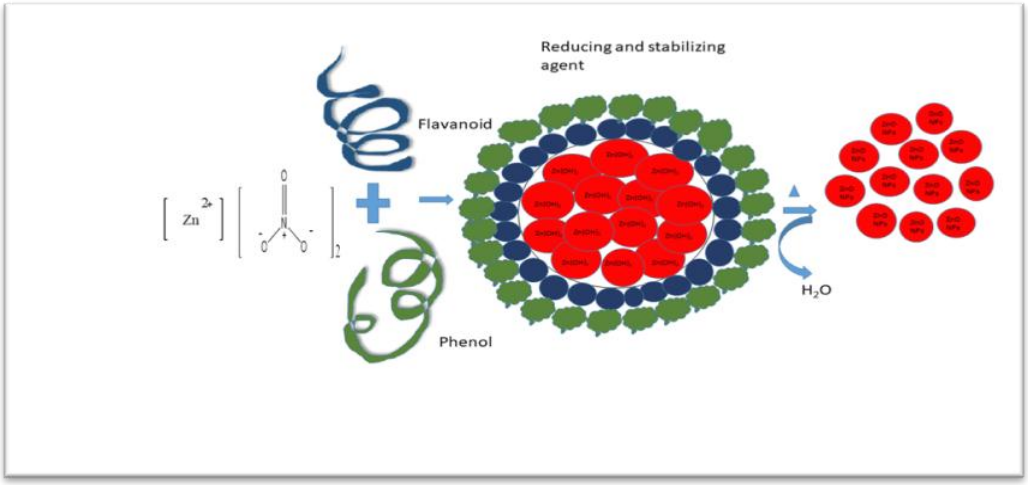

(c)

Fig. 3 FTIR of (a) Chemically synthesized (b) Green synthesized ZnO NPs (c) Scheme of ZnO NPs synthesis through eco-friendly path.

4.4 SEM analysis

The surface morphology of synthesized NPs is shown in Fig. 4.Micrographs of ZnO NPs show how the different synthesis method, and precursors affect the size and shape of the NPs are effected. In bio-mediated NPs, the grain size is regulated and the surface of the substrate is well covered with grains. Size distribution histogram indicated the well distributed nature of synthesized NPs. SEM photos of chemically generated NPs revealed a mostly aggregated structure, whereas bio-fabricated NPs had the flakes-type structure, which can be corroborated with XRD data.[48] Because neem extract contains certain terpenoids, flavonoids the particle size of bio generated NPs (18 nm) is smaller than chemically synthesised NPs (22 nm).[49] As a result, smaller NPs have a greater toxicological effect on bacterial pathogens.

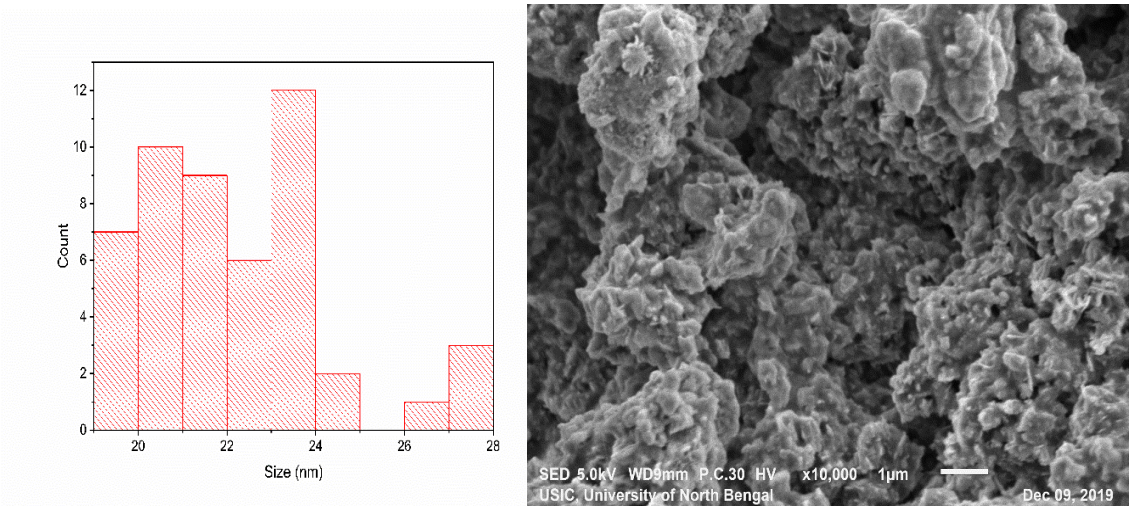

(a)

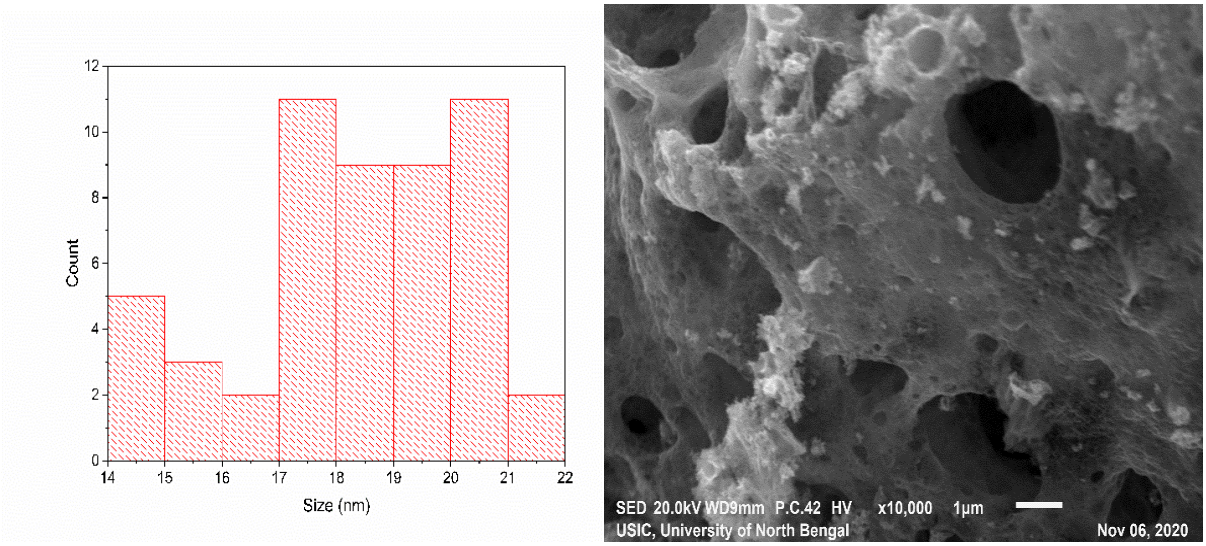

(b)

Fig. 4 SEM images and histrogram of (a) Chemically synthesized (b) Green synthesized ZnO NPs.

4.5 Energy-dispersive X-ray spectroscopy

The EDX plot of SEM images revealed the needed phase of Zn and O, as shown in Fig. 5, and Table 1 represents the atomic % and weight % of products. Zinc of synthesized NPs is shown by the lines between 0-2 k V and 8-10 k V. The appearance of a trace amount of oxygen (0-2 k V) in the EDX spectra indicates the presence of phytochemicals in the plant extract. In a prior study, ZnO NPs were produced from *C. gigantea* leaf extract, and similar peaks were detected.[50]

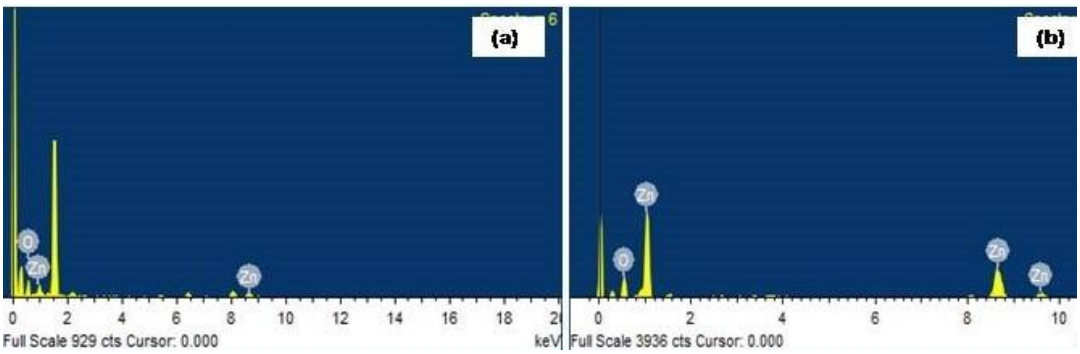

Fig. 5 EDX spectra of (a) Chemically synthesized (b) Green synthesized ZnO NPs.

Table 1: Atomic % and weight % of chemically and green synthesized NPs.

Element	Atomic %	Weight %
Chemically synthesized ZnO NPs	Zn=37.13 O=62.87	Zn=70.70 O=29.30
Green synthesized Zno	Zn=44.85 O=55.15	Zn=76.87 O=23.13

4.6 XRD analysis

XRD study validates the above conclusions even more. The peaks indexed to (100), (002), (101), (102), (110), (103), (112), (201), (202) planes with the space group P63mc and the data compared with JCPDSICDD card: 75–0592 revealed the finger print of hexagonal wurtzite structure. The diffraction angle ranges from 20^0 to 70^0 corresponding to 31.97^0, 34.72^0, 36.65^0, 47.98^0, 56.88^0, 63.06^0, 68.31^0, 69.34^0. The average crystallite size of manufactured NPswas found to be in nm range, as computed using Debye- Scherer equation (Eq. 3).[51]

$$D = k\lambda / \beta \cos \theta \qquad (3)$$

Where k is the Scherer's constant (0.89), λ is the wavelength (1.5406 A^0), β is the full width half maximum (FWHM), θ is Bragg's angle of diffraction. Both the spectrum ensured the formation of ZnO NPs(Fig. 6). The calculated crystalline size of green and chemically synthesized NPs are 20 and 10 nm respectively. The provided data cards (JCPDSICDD card: 75–0592) are in good agreement with the XRD pattern of synthesized NPs, confirming the product's purity, crystallinity, and hexagonal wurtzite structure. No extra peaks of *Azadirachta Indica* laves extract was observed indicating that it was fully immersed into ZnO matrix and improved crystallinity. From literature survey it can be conclude that our synthesis procedure produces smaller bio-synthesized ZnO NPs than others.[52,53] SEM examination reported larger size of nanoparticles than XRD study. So, the small size nanoparticles (10 nm) showed better anti-bacterial activity, indicating the facile method of synthesis of NPs.

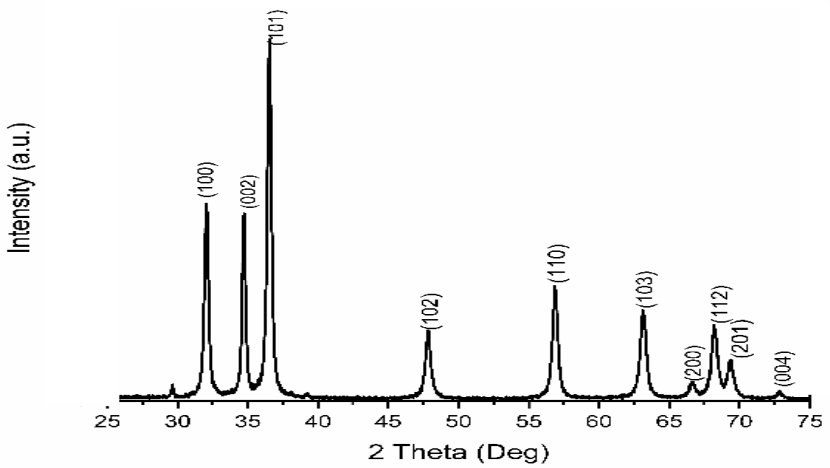

(a)

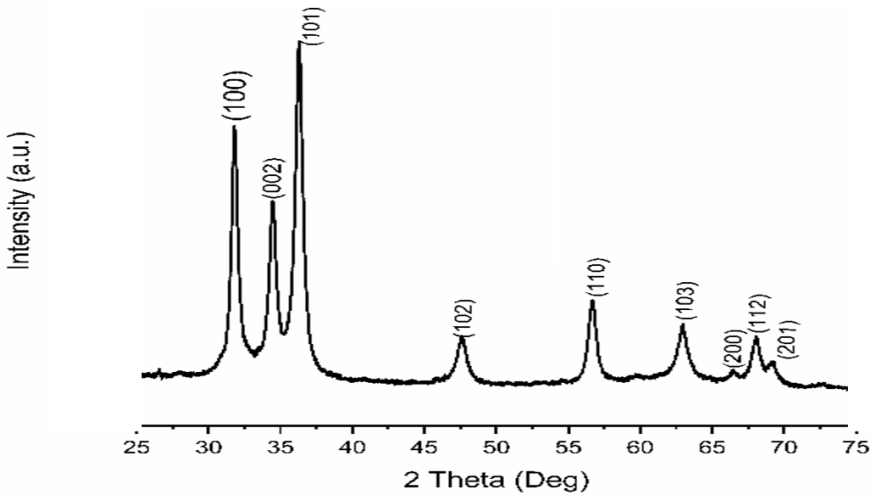

(b)

Fig. 6 XRD pattern of (a) Chemically synthesized (b) Green synthesized ZnO NPs.

4.7 Phytochemical study of *Azadirachta indica*leaves extract responsible for reduction and stabilization of bio-mediated ZnO NPs

It was found that an aqueous extract of neem leaves contains polyphenols and flavonoids (Table 2). According to an FTIR analysis, the alcoholic group of plant extract, which is responsible for the stability of ZnO NPs, shifts by 25 cm^{-1}.[54] Fig. 3c represents the fact of interaction of bioactive components with ZnO NPs, which is further established in the computational analysis. The active components of plant extract, quercetin and sitosterol, reduce Zn^{2+} to ZnO NPs.[55] This is supported by the high interaction energies between quercetin and ZnO NPs. During the bio reduction of ions, gedunin acts as a stabilizing factor.[56]

Table 2: Phytochemical screening of aqueous extract of neem leaves.

Phytochemicals	Leaves extract
Alkaloids	+
Steroids	+
Flavonoids	+
Polyphenols	+
Fatty acids	+
Saponin	+

4.8 Antibacterial activity

The antibacterial activity could be the outcome of following factors (i) electrostatic interactions between the NPs and intercellular species (ii) production of active oxygen species (iii) NPs accumulating into cytoplasm of bacterial cell, disrupting the membrane. The mechanism is that the net positive charge on the surface of ZnO NPs interacts with negative charge of bacteria, promoting the antibacterial action of synthesized NPs. Divya et al., 2013 interpreted the phenomena as production of reactive oxygen species (superoxide, hydroxide radicals) disrupting the cell membrane. Surface oxygen species originated by ZnO NPs restrict the bacterial cell development as reported by Padmavathy and Vijayaraghavan, 2008; Sharma et al., 2010. Fig. 7 represents the mechanism of antibacterial activity schematically.

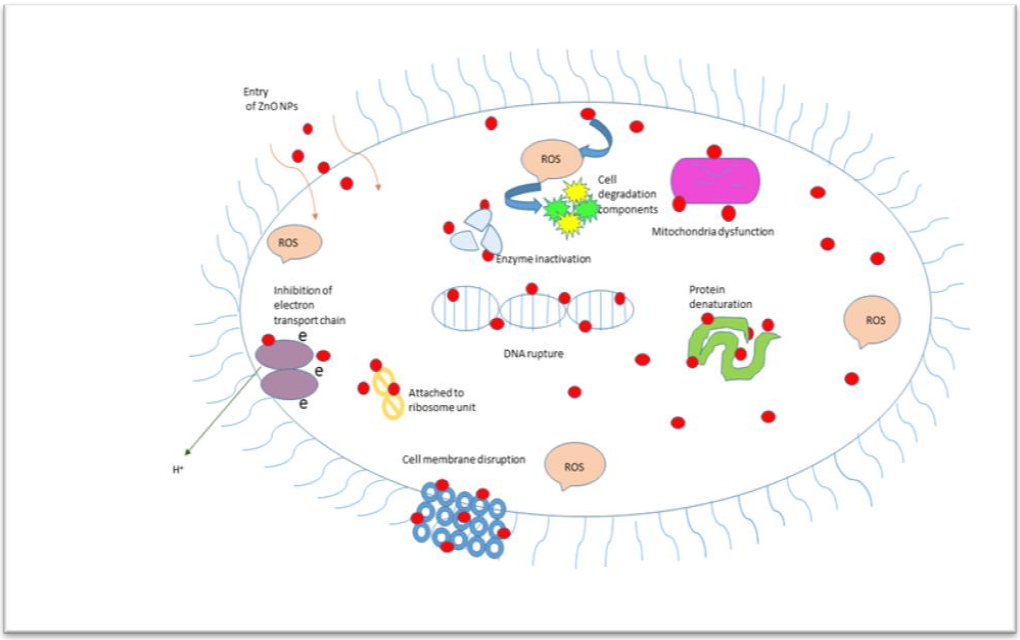

Fig. 7 Schematic representation of various modes of action of ZnO NPs on bacterial cell.

B. subtilis, *Staphylococcus aureus*, *Shigella Sp.* and *E.Coli*were used to test the antibacterial ability of manufactured nanomaterials. The zones of inhibition, as shown in Fig. 8 and Fig. 9, were used to determine the resistance of the following bacteria to nanomaterials and the control antibiotic (ampicillin). It was discovered that the gram positive bacteria were more vulnerable to both NPs and antibiotic than gram negative bacteria. Both the synthesized nanomaterials were shown to be more efficient against *B. subtilis*, with inhibition zones of 28 and 24 mm respectively. The percentage inhibitory potential of PE against *B. subtilis*, *Staphylococcus aureus* and *E. Coli* was noted with

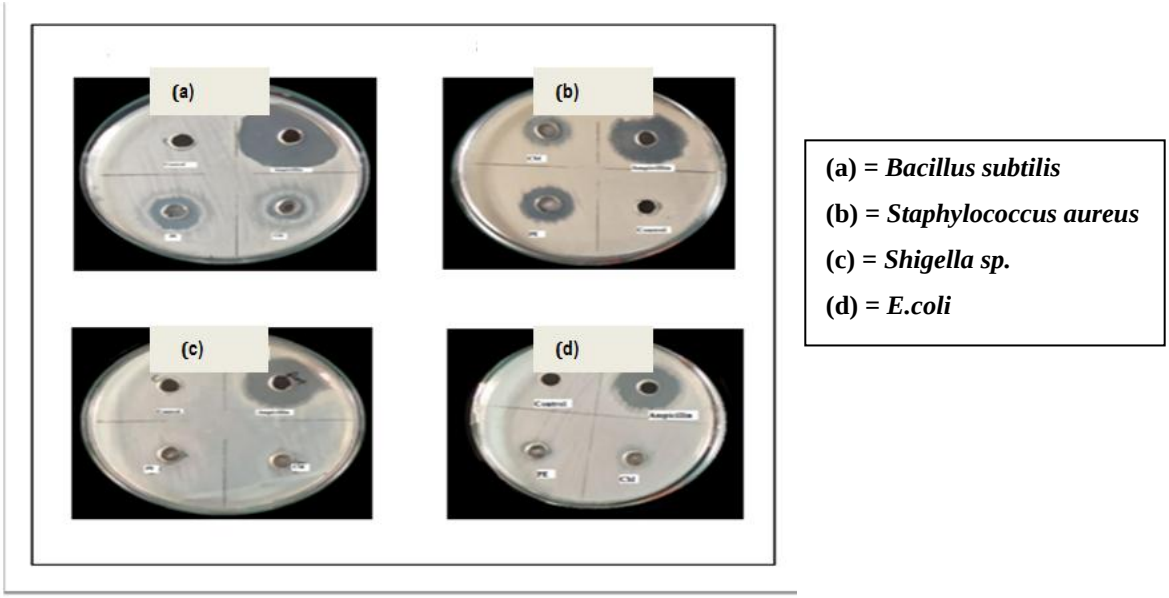

Fig. 8 Antibacterial activity of CM (Chemically synthesized) and PE (green synthesized) ZnO NPs against two gram-positive bacteria and two gram-negative bacteria.

64%, 44% and 23%, but on Shigella, chemically synthesized NPs were more active than bio synthesized NPs which exhibited only 28%. Table 3 represents the antibacterial activity of ZnO NPs synthesized via different methods.

According to previous work, green mediated NPs have stronger antibacterial potential than chemically manufactured NPs because their size is smaller, and the various phytochemicals in plant extracts also play a role in inhibiting bacterial development. Hazardous compounds on the surface of produced NPs may result from chemical synthesis, posing a serious health risk. So, biosynthesized NPs established its potential as a good antibacterial agent.

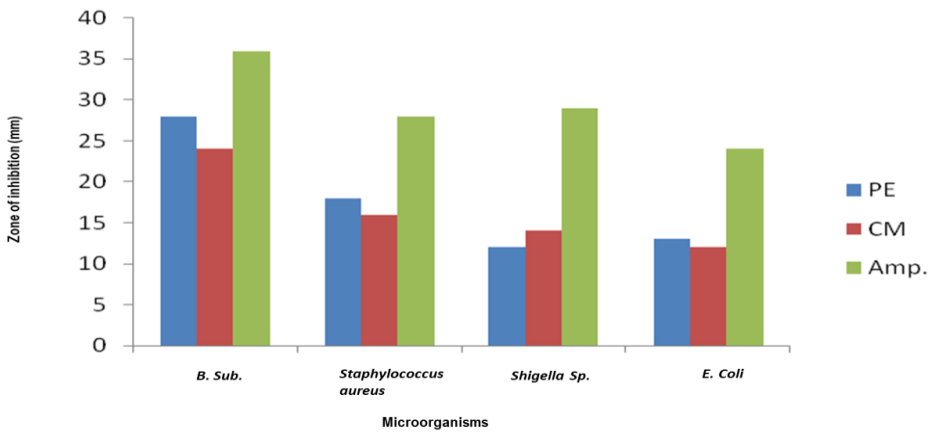

Fig. 9 Zone of inhibition of chemically synthesized (CM) and green synthesized (PE) NPs.

Table 3: Antibacterial activity of ZnO NPs synthesized via chemical, physical and green methods.

SL. No.	Synthesis	Methods	Size (nm)	NPs conc	Zone of inhibition (mm)	Organism	Reference
1	Green	*Melastoma malabathricum*	272	25 mg/mL	8.5	*B. subtilis*	[57]
2	Physical	Spin-coating	34.22	200 mg/mL	15.5	*B. subtilis*	[58]
3	Chemical	Microwave assisted	19	10 µg/mL	19	*B. subtilis*	[39]
4	Green	*Limonia acidissima*	-	400 mg/mL	18	*Shigella Sp.*	[59]
5	Green	*Rauvolfia tetraphylla*	38.16	60 µg/ml	11.4	*Shigella Sp.*	[60]
6	Chemical	Ultrasonication	150-200	5 mg/ml	13	*S. Aureus*	[61]
7	Green	Walnut leaf extract	15-40	10g/50 mL	9	*E. Coli*	[62]
8	Green	C. halicacabum	65	50 µg/ ml	16	*S. Aureus*	[51]

4.9 Quantum chemical studies to explore the reduction behavior of quercetin, β-sitosterol, gedunin

Computational study of three major compounds extracted from *Azadirachta indica* plant extract bearing carbonyl and alcoholic groups were selected for computational study. To understand the detail interaction of the ZnO-NP with these compounds geometry optimizations of these nano composites were carried out. Fig. 10 (a-c) represent the optimized geometries of these nano-composites with ZnO-NP respectively.

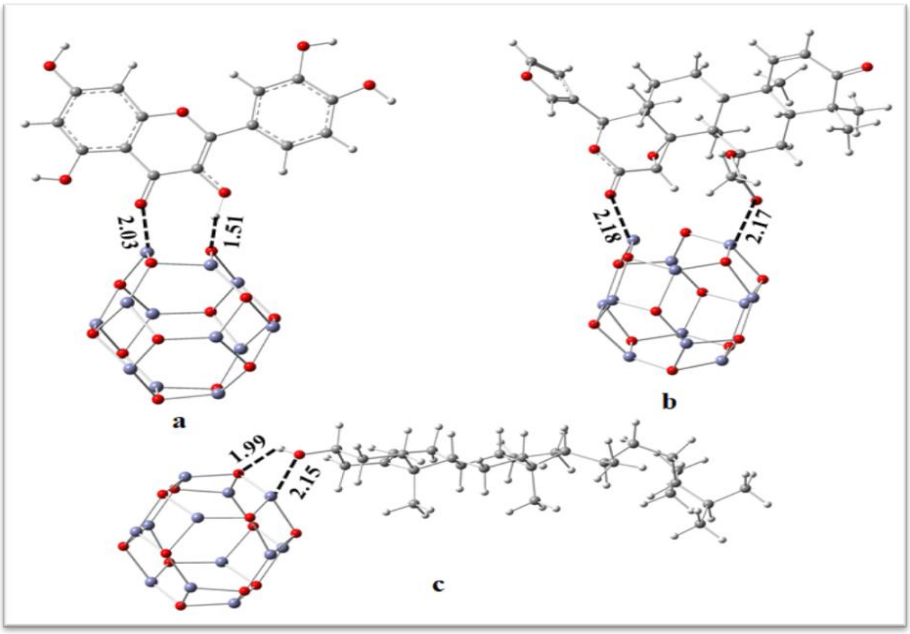

Fig. 10 Optimized geometries of the (a) quercetin-ZnO-NPs, (b) β- sitosterol-ZnO-NPs, (c) gedunin-ZnO-NPs.

A closer look on the optimized geometries revealed that all the three compounds viz. quercetin, β- sitosterol, gedunin form stronger H-bonding which lies within a range of 1.99 to 2.03 angstrom. We have also analyzed the adsorption energies of these nanocomposites and found fairly high adsorption energies of -1.24eV, -35eV,-0.56eV for quercetin, β- sitosterol, gedunin with ZnO NPs respectively. All these data clearly revealed that, ZnO-NP form stronger complex with quercetin molecule.

5. CONCLUSION

Bio-mediated formulation, according with findings of this study, is a preferable alternative to traditional chemical synthesis. In eco-friendly synthesis, the plant extract was utilized to fabricate ZnO NPs while NaOH acts as a reducing agent in second alternative. UV-Vis spectroscopy, FTIR, DLS, SEM, and XRD are used to monitor NPs production. In comparison to chemically assisted ZnO NPs, the crystallinity of smaller size ZnO NPs is improved in eco-friendly method. Both the generated NPs are more effective against gram-positive bacteria. They interact with cell components and change the permeability of the membrane. Chemical synthesis may still result in the presence of hazardous chemicals adsorbed on the surface, which may have bad impacts in health care applications. DFT calculations confirms that among the major components present in neem leaves extract, quercetin exhibits highest interaction energy (-1.24 eV) and mainly responsible for the stabilization of ZnO NPs. As a result, smaller-sized green mediated NPs have a lot of potential in the biological field to be used as a good antibacterial agent instead of traditional medications.

ACKNOWLEDGMENT

The authors gratefully acknowledge UGC, NET-JRF for providing Fellowship, the Department of Chemistry and Bio-Technology, NBU for instrumental assistance.

Declaration of Competing Interest

The authors declare that there is no conflict of interest.

REFERENCES

1. Irshad S, Salamat A, Anjum A A, Sana S, Saleem R S, Naheed A *et al* 2018 *Cogent Chem*., 4: 1469207.
2. Purohit M, Kandwal A, Purohit R, Semwal A, Parveen S, and Khajuria A K 2021 *Asian J. Pharm. Anal*, 11: 275.

3. Mousavi-Khattat M, Keyhanfar M, and Razmjou A 2018 *Artif Cells Nanomed Biotechnol,* 46: S1022.
4. Mohammed Y H, Holmes A, Haridass I N, Sanchez W Y, Studier H, Grice J E *et al* 2019 *J. Investig. Dermatol,* 139308.
5. Gupta M, Tomar R S, Kaushik S, Mishra R K, and Sharma D 2018 *Front. Microbiol,* 92030.
6. Han J, Liu Z, Guo K, Zhang X, Hong T, and Wang B 2015 *J. Power Sources,* 17961.
7. Li X, Zhang F, Ma C, Elingarami S, and He N 2013 *J. Nanosci. Nanotechnol,* 135859.
8. Dobrucka R and Długaszewska J 2016 *Saudi J. Biol. Sci.,* 23517.
9. Tantiwatcharothai S and Prachayawarakorn J 2019 *Int. J. Biol. Macromol,* 135133.
10. Suresh D, Nethravathi P, Rajanaika H, Nagabhushana H, and Sharma S 2015 *Mater. Sci. Semicond. Process,* 31: 446.
11. Steffy K, Shanthi G, Maroky A S, and Selvakumar S 2018 *J Infect* Public Health, 11463.
12. Naik M M, Naik H B, Nagaraju G, Vinuth M, Naika H R, and Vinu K 2019 *Microchem. J.,* 146: 1227.
13. Raja A, Ashokkumar S, Marthandam R P, Jayachandiran J, Khatiwada C P, Kaviyarasu K *et al* 2018 *J. Photochem. Photobiol. B: Biol.,* 18153.
14. Mahendra C, Murali M, Manasa G, Ponnamma P, Abhilash M, Lakshmeesha T *et al* 2017 *Microb. Pathog,* 110620.
15. Ali J, Irshad R, Li B, Tahir K, Ahmad A, Shakeel M *et al* 2018 *J. Photochem. Photobiol. B: Biol,* 183349.
16. Ali K A, Yao R, Wu W, Masum M M I, Luo J, Wang Y *et al* 2020 *Mater. Res. Express,* 7015097.
17. Venkatesan G, Vijayaraghavan R, Chakravarthula S N, and Sathiyan G 2019 *Frontier Research Today,* 22002.
18. Attar A and Yapaoz M A 2018 *Mater. Res. Express,* 5055403.
19. Padalia H, Baluja S, and Chanda S 2017 *BioNano Science,* 740.
20. Shabaani M, Rahaiee S, Zare M, and Jafari S M 2020 *LWT* 134110133.
21. Andrade-Coelho C A, Souza N A, Gouveia C, Silva V C, Gonzalez M S, and Rangel E F 2009 *J. Med. Entomol,* 461125.
22. Srivastava S K, Agrawal B, Kumar A, and Pandey A 2020 *J. Sci. Res.,* 64: 385.
23. Alzohairy M 2016 *Evid.-Based Complementary Altern. Med.,* 201611.
24. Roy P, Das B, Mohanty A, and Mohapatra S 2017 *Appl. Nanosci.,* 7843.

25. Kanase R, Karade V, Kollu P, Sahoo S C, Patil P, Kang S *et al* 2020 *Nano Express,* 1020013.
26. Nagar N and Devra V 2018 *Mater. Chem. Phys.,* 21344.
27. Hareesh K, Williams J, Dhole N, Kodam K, Bhoraskar Vand Dhole S 2016 *Mater. Res. Express,* 3: 075010.
28. Divya R 2020 *Int. Res. J. Adv.* Sci. Hub, 2105.
29. Elumalai K and Velmurugan S 2015 *Appl. Surf. Sci.,* 345329.
30. Bhuyan T, Mishra K, Khanuja M, Prasad R, and Varma A 2015 *Mater. Sci. Semicond. Process,* 3255.
31. Sharma B K, Mehta B R, Shah E V, Chaudhari V P, Roy D R, and Mondal Roy S J 2021 *J. Clust. Sci.,* 198 1.
32. Noorjahan C, Shahina S J, Deepika T, and Rafiq S 2015 *Int. j. sci. res*., 45751.
33. Masoud N, Partsch T, de Jong K P, and de Jongh P E 2019 *Gold Bull.* 52105.
34. Gnanasangeetha D and SaralaThambavani D 2013 *J. Mater. Sci.,* 23206055.
35. Upadhyay P, Jain V K, Sharma S, Shrivastav A, and Sharma R 2020 *Mater. Sci. Eng.,* 798: 012025.
36. Itelima J, Nwokedi V, Ogbonna A, and Nyam M 2016 *World J* Microbiol Biotechnol, 3: 56.
37. Frisch M, Trucks G, Schlegel H, Scuseria G, Robb M, and Cheeseman J *et al* 2016 *Gaussian,* 162.
38. Ghosh N N, Saha S, Pramanik A, Sarkar P, and Pal S 2020 *Comput. Theor. Chem.,* 1182; 112846.
39. Muzaffar S M, Naeem S, Yaseen S, Riaz S, Kayani Z N, and Naseem S 2020 *J. Sol-Gel Sci. Technol,* 9588.
40. Singh A and Kaushik M 2019 *Res. in Physics,* 13102168.
41. Zak A K, Majid W A, Mahmoudian M, Darroudi M, and Yousefi R 2013 *Adv. Powder Technol,* 24: 618.
42. Nagaraju G, Shivaraju G, Banuprakash G, and Rangappa D 2017 *Mater. Today Commun,* 4: 11700.
43. Saware K and Venkataraman A 2014 *J. Clust. Sci.,* 25: 1157.
44. Jain S and Mehata M S 2017 *Sci. Rep.,* 7: 1.
45. Naseer M, Aslam U, Khalid B, and Chen B 2020 *Sci. Rep.,* 10: 1.
46. Ramesh P, Rajendran A, and Ashokkumar M 2022 *Int. J. Environ. Anal. Chem.,* 102: 1.

47. Alamdari S, Sasani Ghamsari M, Lee C, Han W, Park H-H, Tafreshi M *et al* 2020 *app. sciences*, 10: 3620.
48. Devi J S and Bhimba B V 2013 *Int. J. Nanoparticles*, 6: 312.
49. Haque M J, Bellah M M, Hassan M R, and Rahman S 2020 *Nano express*, 1: 010007.
50. Chaudhuri S K and Malodia L 2017 *Appl. Nanosci*, 7: 501.
51. Nithya K and Kalyanasundharam S 2019 *open nano*, 4: 100024.
52. Iqbal Y, Malik A R, Iqbal T, Aziz M H, Ahmed F, Abolaban F A *et al* 2021 *Mater. Lett.*, 305: 130671.
53. Handago D T, Zereffa E A, and Gonfa B A 2019 *open chemistry*, 17: 246.
54. Dutta T, Ghosh N N, Das M, Adhikary R, Mandal V, and Chattopadhyay A P 2020 *J. Environ. Chem. Eng.*, 8: 104019.
55. Pandey G, Verma K, and Singh M 2014 *Int. J. Pharm. Pharm. Sci.*, 6: 444.
56. Aromal S A and Philip D 2012 *Spectrochimica Acta Part A: Molecular and biomolecular Spectroscopy*, 971.
57. Khan M M, Harunsani M H, Tan A L, Hojamberdiev M, Azamay S, and Ahmad N 2020 *BioNano science*, 431499.
58. Sharma N, Kumar J, Thakur S, Sharma S, and Shrivastava V 2013 *Drug Invent. Today*, 5: 50.
59. Murugan M, Rani K B, Wins J A, Ramachandran G, Guo F, and Mothana R A *et al* 2022 *J. King Saud Univ. Sci.*, 34: 101737.
60. Vinay S and Chandrasekhar N 2021 *J. Inorg. Organomet. Polym. Mater.*, 31: 552.
61. Naskar A, Lee S, and Kim K-s 2020 *Pharmaceutics*, 10: 1232.
62. Saemi R, Taghavi E, Jafarizadeh-Malmiri H, and Anarjan N 2021 *Green Process. Synth*, 10: 112.